Diagnosing Multistage Manufacturing Processes With Engineering-Driven Factor Analysis Considering Sampling Uncertainty

Jian Liu
Department Systems and Industrial Engineering,
The University of Arizona,
Tucson, AZ 85721
e-mail: jianliu@email.arizoan.edu

Jionghua Jin
Department Industrial and
Operations Engineering,
The University of Michigan,
Ann Arbor, MI 48109
e-mail: jhjin@umich.edu

A new engineering-driven factor analysis (EDFA) method has been developed to assist the variation source identification for multistage manufacturing processes (MMPs). The proposed method investigated how to fully utilize qualitative engineering knowledge of the spatial variation patterns to guide the factor rotation. It is shown that ideal identification can be achieved by matching the rotated factor loading vectors with the qualitative indicator vectors (IV) that are defined according to spatial variation patterns based on the design constraints. However, the random sampling variability may significantly affect the estimation of the rotated factor loading vectors, leading to the deviations from their true values. These deviations may change the matching results and cause misidentification of the actual variation sources. By using implicit differentiation approach, this paper derives the asymptotic distribution and the associated variance-covariance matrix of the rotated factor loading vectors. Therefore, by considering the effect of sample estimation variability, the variation sources identification problem is reformulated as an asymptotic statistical test of the hypothesized match between the rotated factor loading vectors and the indicator vectors. A real-world case study is provided to demonstrate the effectiveness of the proposed matching method and its robustness to the sample uncertainty. [DOI: 10.1115/1.4024661]

Keywords: implicit differentiation, asymptotic variance-covariance matrix, asymptotic hypothesis testing, variation reduction

1 Introduction

Multistage manufacturing processes (MMPs) are widely used to perform complex manufacturing operations for producing sophisticated products. In such MMPs, there are generally numerous variation sources that potentially contribute to the variations of key product characteristics (KPCs). It is always desirable to conduct the variation reduction by effectively identifying the underlying variation sources for process correction decisions [1]. However, the variation source identification for MMPs is a challenging task due to the complex variation patterns induced by potentially multiple variation sources at different manufacturing stages.

A multistage automotive body assembly process is a typical MMP with numerous KPCs and potential variation sources. For example, as shown in Figs. 1(*a*)–1(*d*), three side-panel parts, Part A, Part B and Part C, are assembled at two stages to form an automotive side aperture. In order to monitor dimensional integrity, 19 quality features (F_1–F_{19}) distributed on the side aperture, are measured. The 38 coordinates of these 19 quality features are defined as the KPCs and their measurements are denoted as $\mathbf{y}$. The variation sources of MMPs are mainly the tooling elements used to locate and join parts and/or subassemblies, including locating pins, clamps, welding-guns, etc. The dimensional deviations of variation sources, denoted as $\mathbf{u}$ in Fig. 1, will cause the deviations of the KPCs from their designated positions. For instance, as shown in Fig. 1(*a*), a positive deviation of the four-way pin P_1 along Z direction will cause the deviation of Part A from its nominal position at stage 1. At stage 2, subassembly A&B has to be reoriented to fit the locating hole on Part A to pin P_5. Thus, the deviations introduced at stage 1 are propagated to stage 2 and the whole subassembly A&B will deviate from its nominal position, even though all the locating pins, P_5–P_8, are perfectly located at their nominal positions. As a result, the first 32 elements of $\mathbf{y}$ that correspond to F_1–F_{16} on subassembly A&B will have nonzero deviations from their nominal values, whereas the last six elements of $\mathbf{y}$ that correspond to F_{17}–F_{19} on Part C will have no deviations. This relationship between variation sources and KPCs can be described by a spatial pattern vector (SPV), $\gamma_{P_{1\_Z}}$, whose first 32 elements are nonzero and its last six elements are zeros. In this case, SPV is denoted as $\gamma_{P_{1\_Z}} = \left[\#_{32}^{\mathrm{T}}\ \mathbf{0}_6^{\mathrm{T}}\right]^{\mathrm{T}}$, where the subscript "$_{P_{1\_Z}}$" indicates the variation source; $\#_{32}$ is a 32×1 vector with all the elements nonzero, and $\mathbf{0}_6$ is a 6×1 zero vector. When the values of elements in $\#_{32}$ are unknown, a SPV can be qualitatively represented as an IV, which sets the elements corresponding to nonzero elements in SPV as 1's and keeps the elements corresponding to zero elements in SPV as 0's. For instance, the IV for $\gamma_{P_{1\_Z}}$ is denoted as $\tau_{P_{1\_Z}}$, where $\tau_{P_{1\_Z}} = \left[\mathbf{1}_{32}^{\mathrm{T}}\ \mathbf{0}_6^{\mathrm{T}}\right]^{\mathrm{T}}$, and $\mathbf{1}_{32}$ is a 32×1 vector with all elements equal to 1.

In this paper, it is assumed that different variation sources will have distinct SPVs. Furthermore, it is assumed that IVs are different from each other, i.e., for a given IV, γ_a, there is at least one different element in any pair of IVs. The different SPVs with the same IVs can be grouped and represented by one single IV. As illustrated in Fig. 1(*b*), a positive deviation of the four-way pin P_3 along Z direction will only affect the KPCs on Part B at stage 1 and their deviations will not be propagated to other parts at stage 2. Thus, the SPV of P_{3_Z} is $\gamma_{P_{3\_Z}} = \left[\mathbf{0}_4^{\mathrm{T}}\ \#_{28}^{\mathrm{T}}\ \mathbf{0}_6^{\mathrm{T}}\right]^{\mathrm{T}}$ and its corresponding IV is $\tau_{P_{3\_Z}} = \left[\mathbf{0}_4^{\mathrm{T}}\ \mathbf{1}_{28}^{\mathrm{T}}\ \mathbf{0}_6^{\mathrm{T}}\right]^{\mathrm{T}}$. The distinctions among SPVs of different variation sources create the basis for variation source identification, which can be conducted by investigating the

Contributed by the Manufacturing Engineering Division of ASME for publication in the Journal of Manufacturing Science and Engineering. Manuscript received December 7, 2012; final manuscript received May 15, 2013; published online July 17, 2013. Editor: Y. Lawrence Yao.

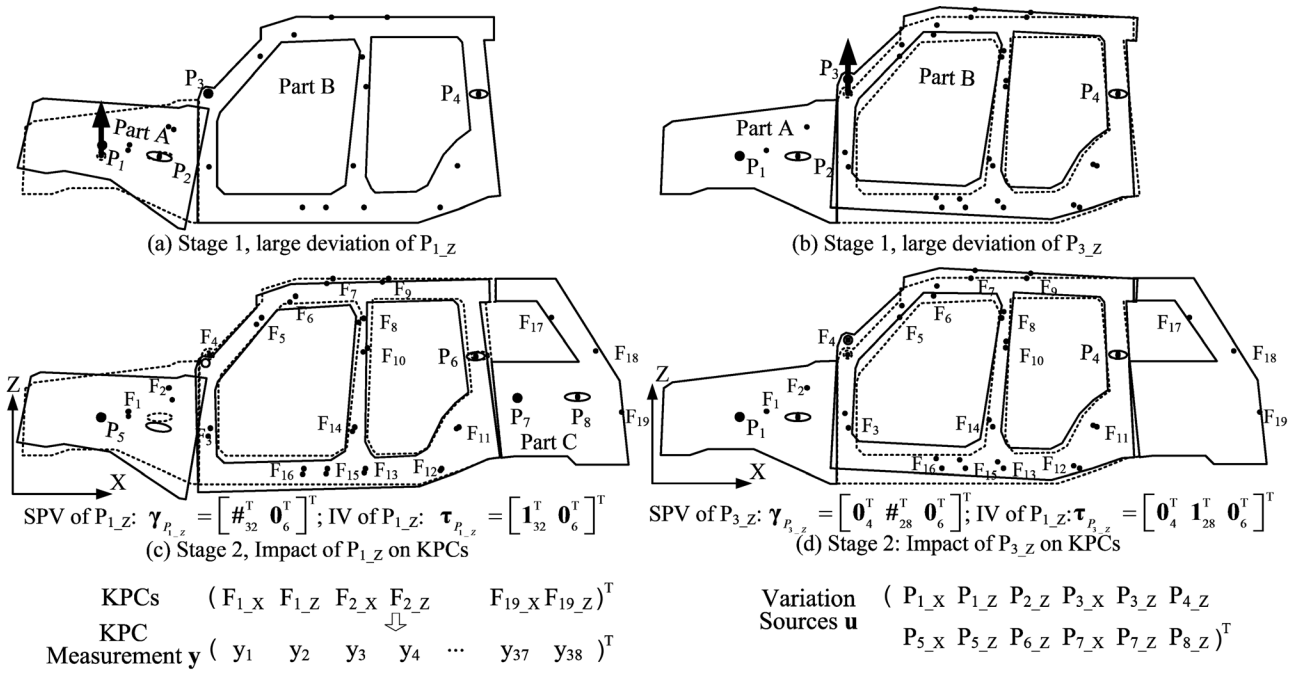

Fig. 1 Illustration of impacts of variation sources on KPCs

SPVs that describe the relationships between KPC measurements, $\mathbf{y}$, and variation sources, $\mathbf{u}$. Such relationships can be defined, by a generic linear model, as

$$\mathbf{y} = \mathbf{\Gamma u} + \mathbf{v} \tag{1}$$

where $\mathbf{y}$ ($\mathbf{y} \in \Re^{p\times 1}$) is a vector of random dimensional deviations of p KPCs. Vector $\mathbf{u}$ ($\mathbf{u} \in \Re^{M\times 1}$) consists of the random deviations of M potential variation sources. The M column vectors in matrix $\mathbf{\Gamma}$ ($\mathbf{\Gamma} \in \Re^{p\times M}$) are the SPVs of the M potential variation sources. Measurement errors are represented by vector $\mathbf{v}$ ($\mathbf{v} \in \Re^{p\times 1}$).

Existing methods for variation source identification in literatures can be classified into two categories: data-driven methods and engineering-driven methods. Data-driven methods do not require a priori engineering knowledge about the relationships between KPC measurements and variation sources. The assumed underlying model is

$$\mathbf{y} = \mathbf{\Gamma}_s \mathbf{u}_s + \mathbf{v} \tag{2}$$

where $\mathbf{y}$ and $\mathbf{v}$ are the same as that defined in Eq. (1). Vector $\mathbf{u}_s$ ($\mathbf{u}_s \in \Re^{s\times 1}$) represents the *s actual variation sources* that present in a MMP and exceed their predefined thresholds. Thus, $\mathbf{u}_s$ is a subset of $\mathbf{u}$ in Eq. (1) and it is assumed that $s < p$. The s column vectors in matrix $\mathbf{\Gamma}_s$ ($\mathbf{\Gamma}_s \in \Re^{p\times s}$) are the SPVs corresponding to the variation sources of $\mathbf{u}_s$. Since no engineering knowledge is presumed, the values of elements in $\mathbf{\Gamma}_s$ are unknown. When the KPC measurements are collected at the final stage of a MMP, the SPVs in $\mathbf{\Gamma}_s$ can be estimated by using Bayesian network analysis [2], principal component analysis [3,4], factor analysis [5,6], and independent component analysis [7]. The variation source identification is implemented by interpreting the estimated SPVs. This approach has two limitations. One limitation is that when multiple actual variation sources present in a MMP, the estimated set of SPVs are not unique, since $s < p$. The other limitation is that the estimated SPVs may sometimes differ from the true SPVs of the actual variation sources due to sample estimation uncertainty. This discrepancy may mislead interpretations and result in misidentification of variation sources.

Engineering-driven methods depend on the derivation of model (1). The values of all SPVs defined in matrix $\mathbf{\Gamma}$ are derived according to the engineering knowledge of nominal product and process design [8–12]. Thus, variances of the elements in $\mathbf{u}$ can be calculated based on the collected KPC measurements $\mathbf{y}$. The elements in $\mathbf{u}$ that have variances larger than predefined thresholds are identified as the actual variation sources [13–18]. In practice, the engineering knowledge needed for deriving model (1) may sometimes be either incomplete or inaccurate. Moreover, the process parameters may sometime deviate from their nominal values. Thus, the model coefficients $\mathbf{\Gamma}$ derived from the *nominal* design may not truly reflect the actual process parameters. Both situations may lead to inaccurate estimation of the variances of the elements in $\mathbf{u}$. As a result, misidentification of the actual variation sources may occur. From this perspective, such an engineering-driven method based on model (1) is not robust to the uncertainty of coefficients in matrix $\mathbf{\Gamma}$.

There is a need for a new systematic approach to identify variation sources by effectively integrating the engineering knowledge represented in a proper form, and in the meantime, taking into account the robustness issue of engineering-driven methods. Liu et al. [19] proposed an EDFA method, where the qualitative engineering knowledge represented by IVs of SPVs is used to guide the factor rotation. Therefore, it has the advantage of estimating the scaled SPVs without requiring an accurate engineering model. However, the primary challenge for implementing such an EDFA, as for other data-driven methods, is how to consider the sample estimation uncertainty. When the sample size of measurement data is small, the rotated factor loading elements estimated from the sample covariance matrix may significantly deviate from their true values. As a result, an estimated loading element may be different from zero even though its true value is zero. For instance, Fig. 2 shows the results of a case study on the MMP illustrated in Fig. 1 (the details will be discussed in Sec. 3). The estimated SPV is given by vector $\hat{\gamma}_k$. The absolute values of those elements, $\#_{\bullet}^{T}$'s, in vector $\hat{\gamma}_k$ are large enough to be considered as nonzero elements. Two predefined IVs are denoted by vectors IV_i and IV_j, of which only three parenthesized elements are different. By comparing only the relative magnitudes of those three corresponding elements in $\hat{\gamma}_k$, it seems that IV_j matches $\hat{\gamma}_k$ better than IV_i as 0.0010 is closer to 0 than −0.0284 and −0.0236. However, the

$$\hat{\boldsymbol{\gamma}}_k:\ \left(0.0010\ \ \#_3^{\mathrm{T}}\ -0.0139\ \ \#_{15}^{\mathrm{T}}\ -0.0135\ \ \#_{11}^{\mathrm{T}}\ -0.0284\ -0.0117\ -0.0236\ -0.0060\ -0.0162\ -0.0047\right)^{\mathrm{T}}$$

$$\mathrm{IV}_i:\ \left(\ (1)\ \ \mathbf{1}_3^{\mathrm{T}}\ \ 1\ \ \mathbf{1}_{15}^{\mathrm{T}}\ \ 1\ \ \mathbf{1}_{11}^{\mathrm{T}}\ \ (0)\ \ 0\ \ (0)\ \ 0\ \ 0\ \ 0\ \right)^{\mathrm{T}}$$

$$\mathrm{IV}_j:\ \left(\ (0)\ \ \mathbf{1}_3^{\mathrm{T}}\ \ 1\ \ \mathbf{1}_{15}^{\mathrm{T}}\ \ 1\ \ \mathbf{1}_{11}^{\mathrm{T}}\ \ (1)\ \ 0\ \ (1)\ \ 0\ \ 0\ \ 0\ \right)^{\mathrm{T}}$$

Fig. 2 Matching of estimated SPV with IVs

actual variation source in that process is P_{1_Z}, which corresponds to IV_i, rather than IV_j. This misidentification demonstrates the essential need to consider sample estimation uncertainty on EDFA for variation source identification.

In this paper, a new method is proposed to explicitly consider the sample estimation uncertainty of EDFA for variation sources identification, which is performed by formulizing an asymptotic statistical testing on the hypothesized match between the rotated factor loading vectors and the predefined IVs. It will be demonstrated that the proposed method will have the advantage of improving the existing EDFA by reducing the misidentification rate, especially when the sample size is small.

The remainder of this paper will be organized as follows: Section 2 presents the proposed methodology with the development of its associated three functional modules, in which the major effort is devoted to the derivation of the asymptotic variance–covariance matrix of the factor loading elements estimated by the EDFA. The procedure of variation source identification based on the asymptotic statistical testing is also introduced. Section 3 demonstrates the effectiveness of the proposed methodology with a case study. Conclusions and future works are discussed in Sec. 4.

2 Methodology

The proposed methodology is based on the assumed model (2). In this paper, the following assumptions are made for this model: (i) $\mathbf{y}$ represents the observable KPC measurements, following p-dimensional normal distribution, i.e., $\mathbf{y} \sim N_p(\boldsymbol{\mu}_\mathbf{y}, \boldsymbol{\Sigma}_\mathbf{y})$. Without loss of generality, it is assumed that $\boldsymbol{\mu}_\mathbf{y} = \mathbf{0}$ under the normal working condition; (ii) $\mathbf{u}_s$ ($\mathbf{u}_s = [u_1, u_2, \ldots, u_s]^{\mathrm{T}}$) represents the actual variation sources, following s-dimensional ($1 < s < p$) normal distribution, i.e., $\mathbf{u}_s \sim N_s(\mathbf{0}, \boldsymbol{\Sigma}_{\mathbf{u}_s})$; (iii) it is reasonable to assume that $\boldsymbol{\Sigma}_{\mathbf{u}_s}$ is a diagonal matrix because that variation sources, e.g., fixture locating pins, are often fabricated, installed and maintained separately for different stations and thus are independent of each other; (iv) $\boldsymbol{\Gamma}_s (\boldsymbol{\Gamma}_s = [\boldsymbol{\gamma}_1\ \boldsymbol{\gamma}_2 \ldots \boldsymbol{\gamma}_s])$ is an *unknown* constant $p \times s$ matrix, with column vector $\boldsymbol{\gamma}_r$ being the true SPV that represents the linear impacts of u_r on $\mathbf{y}$, $r = 1, 2, \ldots, s$; and (v) the measurement errors represented by $\mathbf{v}$ are independent of the variation sources $\mathbf{u}_s$, and follow a p-dimensional normal distribution, i.e., $\mathbf{v} \sim N_p(\mathbf{0}, \boldsymbol{\Sigma}_\mathbf{v})$. It is assumed that measurement errors are independent of each other and have the same variance magnitude, i.e., $\boldsymbol{\Sigma}_\mathbf{v} = \sigma^2 \mathbf{I}_p$, where σ^2 is a constant scalar and $\mathbf{I}_p$ is a $p \times p$ identity matrix.

The proposed variation identification method is developed with three functional modules, including (i) estimating the scaled SPVs with the rotated factor loading vectors derived by EDFA, (ii) evaluating asymptotic variability of the rotated factor loading vectors, and (iii) testing the hypothesized match to identify the actual variation sources. The details of each module will be discussed in Secs. 2.1–2.3.

2.1 Basis of Engineering-Driven Factor Analysis With Sample Data. The objective of the EDFA method is to estimate scaled $\boldsymbol{\gamma}_r$'s, $r = 1, \ldots, s$, without directly measuring $\mathbf{u}_s$ [19]. The sample covariance matrix of KPC measurements, $\mathbf{y}$, can be approximated with the eigen-decomposition as

$$\mathbf{S}_\mathbf{y} \cong \hat{\mathbf{L}}\hat{\mathbf{L}}^{\mathrm{T}} + \mathbf{S}_\mathbf{v} = \hat{\mathbf{E}}_s \hat{\boldsymbol{\Lambda}}_s \hat{\mathbf{E}}_s^{\mathrm{T}} + \hat{\sigma}^2 \mathbf{I}_p \tag{3}$$

where the estimate of initial loading matrix $\hat{\mathbf{L}}$ is defined as

$$\hat{\mathbf{L}} = [\hat{\mathbf{l}}_1\ \hat{\mathbf{l}}_2\ \ldots\ \hat{\mathbf{l}}_s] = \hat{\mathbf{E}}_s \hat{\boldsymbol{\Lambda}}_s^{1/2} \tag{4}$$

$\hat{\boldsymbol{\Lambda}}_s = \mathrm{diag}\{\hat{\lambda}_1, \hat{\lambda}_2, \ldots, \hat{\lambda}_s\}$ and $\hat{\mathbf{E}}_s = [\hat{\mathbf{e}}_1\ \hat{\mathbf{e}}_2\ \ldots\ \hat{\mathbf{e}}_s]$; $\hat{\lambda}_r$'s and $\hat{\mathbf{e}}_r$'s, $r = 1, \ldots, s$, are the s largest eigenvalues and their associated eigenvectors of $\mathbf{S}_\mathbf{y}$, with $\hat{\lambda}_1 \geq \hat{\lambda}_2 \geq \cdots \geq \hat{\lambda}_s > \hat{\sigma}^2$; s is the number of actual variation sources and is determined by Akaike Information Criterion (AIC) [5]; $\hat{\sigma}^2$ is the estimate of the variance of measurement errors. $\hat{\mathbf{l}}_r$'s are the eigenvalue-normed eigenvectors [20], i.e.,

$$\hat{\mathbf{l}}_r = \sqrt{\hat{\lambda}_r}\hat{\mathbf{e}}_r, \quad r = 1, 2, \ldots s \tag{5}$$

It has been shown that that the SPVs of the variation sources are imbedded in the measurement data and span the same linear space of the eigenvectors of $\boldsymbol{\Sigma}_\mathbf{y}$, i.e., $\mathrm{span}\{\mathbf{l}_1\ \mathbf{l}_2\ \ldots\ \mathbf{l}_s\} = \mathrm{span}\{\boldsymbol{\gamma}_1\ \boldsymbol{\gamma}_2\ \ldots\ \boldsymbol{\gamma}_s\}$ [21], where $\mathbf{l}_r$'s are the eigenvalue-normed eigenvectors of the population covariance matrix $\boldsymbol{\Sigma}_\mathbf{y}$. $\mathbf{l}_r$'s can be consistently estimated by $\hat{\mathbf{l}}_r$'s defined in Eq. (5).

For variation source identification, the objective of factor rotation is to obtain the right loading structures that best estimate the scaled SPVs. Assume there are M potential variation sources, each of which has an IV denoted as $\boldsymbol{\tau}_m$, $m = 1, \ldots, M$. As aforementioned, an IV consists of *restricted elements* (i.e., elements equal to 0) and *unrestricted elements* (i.e., elements equal to 1). When the number of variation sources s is determined based on AIC, a combination of s IVs will be selected to form an indicator matrix, $\mathbf{T}_c$, where $\mathbf{T}_c = (\tau_{ir}^c)$, $i = 1, 2, \ldots, p$, $r = 1, 2, \ldots, s$, $c = 1, 2, \ldots, C$. C is the total number of possible IV combinations with $C = \binom{M}{s}$, i.e., C is the number of possible ways to select s IVs from that of M potential variation sources. The indicator matrix of combination c will be used to guide the factor rotation and obtain the corresponding rotated factor loading matrix $\hat{\mathbf{L}}_c^*$, where

$$\hat{\mathbf{L}}_c^* = h_c(\hat{\mathbf{L}}) = \hat{\mathbf{L}}\mathbf{R}_c = [\hat{\mathbf{l}}_{1,c}^*\ \hat{\mathbf{l}}_{2,c}^*\ \ldots\ \hat{\mathbf{l}}_{s,c}^*] = (\hat{l}_{ir,c}^*) \tag{6}$$

Liu et al. [19] developed the *indicator-vector-guided factor rotation* (IVGFR) technique by introducing the concept of *restricted loading element* as follows (Chap. 6 of Ref. [22]).

DEFINITION 1. *For a rotated factor loading matrix* $\hat{\mathbf{L}}_c^*$, *a restricted loading element is defined as an element*, $\hat{l}_{ir,c}^*$, *that corresponds to a restricted element*, τ_{ir}^c, *in* $\mathbf{T}_c$, *where* $\tau_{ir}^c = 0$.

The determination of the rotation matrix $\mathbf{R}_c$ of a given IV combination c, is formulated as an optimization problem to find an optimal $\mathbf{R}_c$ to minimize the sum of square of the restricted loading elements, and at the same time, keep the norm of the loading vectors unchanged. The optimal solution of $\mathbf{R}_c$ can be obtained by applying Lagrangian multiplier method, i.e.,

$$\underset{\mathbf{R}_c}{\mathrm{argmin}}\quad 2Q_c = \sum_{r=1}^{s}\sum_{i=1}^{p}\left((1 - \tau_{ir}^c)\cdot \hat{l}_{ir,c}^*\right)^2 - \sum_{r=1}^{s}\alpha_{r,c}\left(\sum_{i=1}^{p}\left(\hat{l}_{ir,c}^{*2} - \hat{l}_{ir}^2\right)\right) \tag{7}$$

where $\alpha_{r,c}$ is the Lagrangian multiplier to determine the weight for the rth column of $\mathbf{R}_c$. The detail procedure for solving $\mathbf{R}_c$ in Eq. (7) can be found in Ref. [19]. When the combination of IVs in $\mathbf{T}_c$

belongs to the actual variation sources, Q_c will be ideally equal to zero.

Since the rotated loading vectors, $\hat{\mathbf{l}}^*_{r,c}$'s, are estimated from $\mathbf{S_y}$, these vectors will randomly deviate from $\mathbf{l}^*_{r,c}$'s, which are derived from the eigenvalue-normed eigenvectors, $\mathbf{l}_r$'s, of the population covariance matrix $\mathbf{\Sigma_y}$. This type of deviations may make the restricted loading elements in $\hat{\mathbf{l}}^*_{r,c}$'s not exactly equal to zero, and thus Q_c calculated by using the correct IV combination (associated to the actual variation sources) may deviate from its ideal zero value and may sometimes be even larger than another $Q_{c'}$ calculated from a wrong IV combination. This indicates that the sample induced variability of $\hat{\mathbf{l}}^*_{r,c}$'s may lead to misidentification of the actual variation sources, and such a misidentification rate will deteriorate as the sample size is decreased. Therefore, it is essential to develop a new variation sources identification method that is robust to the sampling uncertainty of the rotated factor loading elements.

2.2 Asymptotic Distribution of Factor Loadings. The underlying statistical issue of the proposed variation source identification is to determine, based on sample data, whether the zero Q_c is tenable in the population model. Equivalently, it is to determine whether the restricted loadings elements defined in Definition 1 are statistically equal to zeros. For instance, a small loading element in $\hat{\mathbf{L}}^*_c$, such as 0.0010, may be significantly different from zero if its corresponding standard error is also small. Thus, it is essential to estimates the sampling variability of the rotated factor loading elements. In a landmark series of articles, Jennrich and his colleagues proposed the general framework for deriving the asymptotic standard errors of rotated factor loading elements [23–25]. In this paper, this framework is adopted to analytically derive the asymptotic variance–covariance matrix of the factor loading elements obtained from IVGFR as formulated in Eq. (7).

For a specific IV combination c, $c = 1,2,\ldots, C$, the *true* rotated factor correlation matrix is define as $\mathbf{\Phi}_c = (\phi_{uv,c})$, where

$$\mathbf{\Phi}_c = \left(\mathbf{R}_c^{\mathrm{T}}\mathbf{R}_c\right)^{-1} \tag{8}$$

and $u,v = 1, 2,\ldots, s$. It should be noted that $\mathbf{\Phi}_c$ is a function of $\hat{\mathbf{L}}$, since the rotation matrix is based on $\hat{\mathbf{L}}$ defined in Eq. (4). As matrix $\mathbf{\Phi}_c$ is a *correlation* matrix, its diagonal elements must be equal to 1, i.e.,

$$\mathrm{diag}(\mathbf{\Phi}_c) = \mathbf{I} \tag{9}$$

where the function diag($\mathbf{A}$) keeps the diagonal elements of a square matrix $\mathbf{A}$ and sets all its off-diagonal elements to zeros.

Assuming that h_c has a differential dh_c at $\mathbf{L}$, the *true* initial loading matrix, then dh_c is a linear transformation that maps $p \times s$ matrices into $p \times s$ matrices and this linear mapping approximates h_c at $\mathbf{L}$. It is noted that this true initial loading matrix is derived from the eigenvectors and eigenvalues of the *population* covariance matrix of $\mathbf{y}$, as similarly defined in Eq. (4). Based on the standard asymptotic theory, it yields

$$\sqrt{n}\left(\hat{\mathbf{L}}^*_c - \mathbf{L}^*_c\right) \overset{a}{=} dh_c\left(\sqrt{n}\left(\hat{\mathbf{L}} - \mathbf{L}\right)\right) \tag{10}$$

where "$\overset{a}{=}$" indicates that the difference between the two sides of Eq. (10) approaches zero in probability "1" as the sample size n approaches infinity. $\mathbf{L}^*_c$ is the *true* rotated factor loading matrix and $\hat{\mathbf{L}}^*_c$ is its asymptotically normal estimate. The asymptotic variance–covariance matrix of $\hat{\mathbf{L}}^*_c$ can be obtained from that of $\hat{\mathbf{L}}$. In terms of the partial derivatives of the function h_c

$$\mathrm{acov}(\hat{l}^*_{ir,c}, \hat{l}^*_{jq,c}) = \sum_{mnxy} \frac{\partial h_{ir,c}}{\partial \hat{l}_{mx}} \mathrm{acov}(\hat{l}_{mx}, \hat{l}_{ny}) \frac{\partial h_{jq,c}}{\partial \hat{l}_{ny}}, \quad i,j,m,n = 1,2,\ldots,p, \text{ and } r,q,x,y = 1,2,\ldots,s \tag{11}$$

where $\mathrm{acov}(\hat{l}_{mx}, \hat{l}_{ny})$ is the asymptotic covariance between two elements of the initial factor loading vectors (defined in Eq. (5)). It has been given by Girshick [26] as

$$\mathrm{acov}(\hat{l}_{mx}, \hat{l}_{ny}) = \frac{\hat{\lambda}_y \hat{\lambda}_x \hat{l}_{my} \hat{l}_{nx}}{n(\hat{\lambda}_x + \xi_{xy}\hat{\lambda}_y)(\hat{\lambda}_y + \xi_{xy}\hat{\lambda}_x)} + \frac{\hat{\lambda}_x^2 \delta_{xy}}{n} \sum_{t=1}^{p} \frac{\hat{l}_{mt}\hat{l}_{nt}}{(\hat{\lambda}_x + \xi_{xt}\hat{\lambda}_t)(\hat{\lambda}_y + \xi_{yt}\hat{\lambda}_t)} \tag{12}$$

and

$$\delta_{xy} = \begin{cases} 1, & \text{if } x = y \\ 0, & \text{if } x \neq y \end{cases} \quad \text{and} \quad \xi_{xy} = \begin{cases} 1, & \text{if } x = y \\ -1, & \text{if } x \neq y \end{cases} \tag{13}$$

The partial derivative $\partial h_{ir,c}/\partial \hat{l}_{jq}$ is needed to evaluate the asymptotic variances and covariance of $\hat{l}^*_{ir,c}$'s. For the factor rotation, function h_c is a straightforward linear function transforming $\hat{\mathbf{L}}$ to $\hat{\mathbf{L}}^*_c$ with rotation matrix $\mathbf{R}_c$, as similarly defined in Eq. (6). However, according to the IVGFR algorithm, $\mathbf{R}_c$ itself is also the result of an implicit function of $\hat{\mathbf{L}}$. Thus, the function h_c is not given explicitly in terms of $\hat{\mathbf{L}}$ and it is difficult to explicitly derive its partial derivatives with respect to $\hat{l}_{ir}$'s. In this paper, those partial derivatives will be derived by means of the implicit differentiation as follows. Suppose that

$$\boldsymbol{\psi}_c = \boldsymbol{\psi}(\hat{\mathbf{L}}^*_c, \mathbf{\Phi}_c) = \mathbf{0} \tag{14}$$

where $\boldsymbol{\psi}_c = (\psi_{uv,c})$ is an $s(s\text{-}1)$-dimensional constraint being satisfied by rotation function h_c. We can differentiate the relationships defined in Eqs. (6), (8), (9), and (14) to get $d\hat{\mathbf{L}}^*_c$ in terms of $d\hat{\mathbf{L}}$. The solution will define the differential dh_c. The required partial derivatives of h_c with respect to an initial factor loading elements in $\hat{\mathbf{L}}$ is defined in the coordinate form as

$$\partial h_{ir,c}/\partial \hat{l}_{jq} = dh_{ir,c}(\mathbf{J}(j,q)) \tag{15}$$

where $\mathbf{J}(j,q)$ is an elementary $p \times s$ matrix whose (j,q)th element is one and other elements are zeros. In a matrix form, Eq. (15) can also be written as

$$\mathbf{H}_c = \left(\partial h_{ir,c}/\partial \hat{l}_{jq}\right) \tag{16}$$

where $\mathbf{H}_c$ is a $ps \times ps$ matrix whose column index and row index are defined according to the lexicographic order. Jennrich [24] viewed the general solution of dh_c as a composition of four linear transformations and expressed the matrix $\mathbf{H}_c$ in the form of

$$\mathbf{H}_c = \mathbf{B}_c - \mathbf{C}_c\mathbf{D}_c^{-1}\mathbf{E}_c \tag{17}$$

$\mathbf{B}_c$ is a $ps \times ps$ matrix defined as

$$\mathbf{B}^c_{ir,jq} = \delta_{ij}\mathbf{R}_{qr,c} \tag{18}$$

where δ_{ij} is a Kronecker delta and $\mathbf{R}_{qr,c}$ is the (q,r)th element of rotation matrix $\mathbf{R}_c$. $\mathbf{C}_c$ is a $ps \times ss$ matrix whose elements are defined as

$$\mathbf{C}^c_{ir,uv} = \hat{l}^*_{iu,c}\phi^{vr,c} \tag{19}$$

where $\hat{l}^*_{iu,c}$ is the (i,u)th element of $\hat{\mathbf{L}}^*_c$ and $\phi^{vr,c}$ is the (v,r)th element of $\mathbf{\Phi}_c^{-1}$. $\mathbf{D}_c$ is an $ss \times ss$ matrix defined as

$$\mathbf{D}^c_{uv,xy} = \sum_{i=1}^{p}\sum_{r=1}^{s} \frac{\partial \psi_{uv,c}}{\partial \hat{l}^*_{ir,c}} \hat{l}^*_{ix,c}\phi^{yr,c} - \frac{\partial \psi_{uv,c}}{\partial \phi_{xy,c}} - \frac{\partial \psi_{uv,c}}{\partial \phi_{yx,c}} \tag{20}$$

where $\partial\psi_{uv,c}/\partial\hat{l}^*_{ir,c}$ and $\partial\psi_{uv,c}/\partial\phi_{xy,c}$ are defined by the constraint $\boldsymbol{\psi}_c$ and are rotation algorithm specific. $\mathbf{E}_c$ is an $ss \times ps$ matrix defined as

$$\mathbf{E}^c_{xy,jq} = \sum_{r=1}^{s} \frac{\partial\psi_{xy,c}}{\partial\hat{l}^*_{jr,c}} \mathbf{R}_{qr,c} \tag{21}$$

Since the constraint $\boldsymbol{\psi}_c$ is a function of $\hat{\mathbf{L}}^*_c$ and $\mathbf{R}_c$, it depends on the specific rotation algorithm used. In the coordinate form, it is defined as

$$\psi_{uv,c} = \sum_{i=1}^{p}\sum_{r=1}^{s} \frac{\partial Q_c}{\partial\hat{l}^*_{ir,c}} \cdot \hat{l}^*_{iu,c} \cdot \phi^{vr,c} \tag{22}$$

where Q_c is the optimization index used in finding the rotation matrix $\mathbf{R}_c$, $\phi^{vr,c}$ is the (v,r)th element of matrix $\boldsymbol{\Phi}_c^{-1}$. For IVGFR used in this paper, Q_c is given in formulation (7) for a specific IV combination c. Thus, the partial derivative of Q_c is

$$\frac{\partial Q_c}{\partial l^*_{ir,c}} = \left(\left(1-\tau^c_{ir}\right)^2 - \alpha_{r,c}\right) \cdot \hat{l}^*_{ir,c} \tag{23}$$

Thus, from Eqs. (22) and (23), the constraint functions in the coordinate form are

$$\psi_{uv,c} = \sum_{i=1}^{p}\sum_{r=1}^{s} \left(\left(1-\tau^c_{ir}\right)^2 - \alpha_{r,c}\right) \cdot \hat{l}^*_{ir,c} \cdot \hat{l}^*_{iu,c} \cdot \phi^{vr,c} \tag{24}$$

And their partial derivatives can be derived as

$$\frac{\partial\psi_{uv,c}}{\partial\hat{l}^*_{ir,c}} = \delta_{ur}\left(\frac{\partial Q_c}{\partial\hat{\mathbf{L}}^*_c}\boldsymbol{\Phi}_c^{-1}\right)_{iv} + \left(\left(1-\tau^c_{ir}\right)^2 - \alpha_{r,c}\right) \cdot \hat{l}^*_{iu,c} \cdot \phi^{vr,c}, \text{ and} \tag{25}$$

$$\frac{\partial\psi_{uv,c}}{\partial\phi_{xy,c}} = -\sum_{i=1}^{p}\sum_{r=1}^{k} \left(\left(1-\tau^c_{ir}\right)^2 - \alpha_{r,c}\right) \hat{l}^*_{ir,c}\hat{l}^*_{iu,c}\phi^{rx,c}\phi^{yv,c} \tag{26}$$

The partial derivatives of the constraints defined in Eqs. (25) and (26) can be plugged into $\mathbf{C}_c$ and $\mathbf{D}_c$ to get partial derivatives of h_c, as defined in Eq. (16). Then, the elements of $\mathbf{H}_c$ will be used in Eq. (11) to calculate the asymptotic variance–covariance of $\hat{l}^*_{ir,c}$'s. For a given $\mathbf{T}_c$, it is easy to define

$$\hat{\boldsymbol{\eta}}^*_c = \text{vec}(\hat{\mathbf{L}}^*_c) \tag{27}$$

where $\hat{\boldsymbol{\eta}}^*_c \in \Re^{ps\times 1}$ and is ps-dimensional asymptotically normally distributed with the mean at its own *true* vector, $\boldsymbol{\eta}^*_c$, and the asymptotic covariance matrix as

$$\Sigma^c_{\boldsymbol{\eta}} = \left(\text{acov}(\hat{l}^*_{ir,c}, \hat{l}^*_{jq,c})\right) \tag{28}$$

i.e., $\hat{\boldsymbol{\eta}}^*_c \sim N_{ps}(\boldsymbol{\eta}^*_c, \boldsymbol{\Sigma}^c_{\boldsymbol{\eta}})$, where $\boldsymbol{\Sigma}^c_{\boldsymbol{\eta}} \in \Re^{ps\times ps}$.

2.3 Statistical Testing for Variation Source Identification. The variation source identification based on EDFA is implemented by checking the hypothesized match between the restricted loading elements and the restricted elements in IVs. The potential variation sources whose IVs achieve the best match are identified as the actual variation sources. Liu et al. [19] evaluated this match by Q_c but did not consider the impact of sampling uncertainty. Because both the asymptotic distributions and the variance–covariance matrix of all $\hat{l}^*_{ir,c}$'s have been derived, the hypothesized match can be formulated as a statistical test with respect only to those restricted loading elements.

DEFINITION 2. *for a given* $\mathbf{T}_c$, a *restricted loading vector* is *defined as*

$$\underset{\sim}{\hat{\boldsymbol{\eta}}}^*_c = \mathbf{S}_c \cdot \hat{\boldsymbol{\eta}}^*_c \tag{29}$$

where $\underset{\sim}{\hat{\boldsymbol{\eta}}}^*_c \in \Re^{W_c\times 1}$, W_c *is the number of restricted elements in* $\boldsymbol{\tau}_c$, *and* $\boldsymbol{\tau}_c = \text{vec}(\mathbf{T}_c)$. $\mathbf{S}_c$ *is a selection matrix and its* (w, t)th *element is 1 if the* wth *element of* $\boldsymbol{\tau}_c$ *is the* tth *zero in* $\boldsymbol{\tau}_c$, *where* $w = 1, 2,\ldots,$ W_c, *and* $t = 1, 2,\ldots, ps$. *Other elements in* $\mathbf{S}_c$ *are zeros.*

With the manipulation defined in Eq. (29), $\underset{\sim}{\hat{\boldsymbol{\eta}}}^*_c$ will be a vector that contains only the restricted loading elements in $\hat{\mathbf{L}}^*$. $\underset{\sim}{\hat{\boldsymbol{\eta}}}^*_c$ follows a W_c-dimensional asymptotic normal distribution with the mean at its *true* vector, $\underset{\sim}{\hat{\boldsymbol{\eta}}}^*_c$, and the asymptotic variance–covariance matrix as

$$\underset{\sim}{\Sigma}^c_{\boldsymbol{\eta}} = \mathbf{S}_c\boldsymbol{\Sigma}^c_{\boldsymbol{\eta}}\mathbf{S}_c^{\mathrm{T}} \tag{30}$$

i.e., $\underset{\sim}{\hat{\boldsymbol{\eta}}}^*_c \sim N_{W_c}(\underset{\sim}{\boldsymbol{\eta}}^*_c, \underset{\sim}{\boldsymbol{\Sigma}}^c_{\boldsymbol{\eta}})$, where $\underset{\sim}{\boldsymbol{\Sigma}}^c_{\boldsymbol{\eta}} \in \Re^{W_c\times W_c}$.

For a given $\mathbf{T}_c$, the matching between the restricted loading elements and the restricted elements is formulated as a hypothesis test, i.e.,

$$\begin{aligned} H^c_0 &: \underset{\sim}{\boldsymbol{\eta}}^*_c = \mathbf{0} \text{ versus} \\ H^c_a &: \underset{\sim}{\boldsymbol{\eta}}^*_c \neq \mathbf{0} \end{aligned} \tag{31}$$

When H^c_0 is true, the limiting distribution of the test statistic ω_c

$$\omega_c = \underset{\sim}{\hat{\boldsymbol{\eta}}}^{*\mathrm{T}}_c \left(\underset{\sim}{\boldsymbol{\Sigma}}^c_{\boldsymbol{\eta}}\right)^{-1} \underset{\sim}{\hat{\boldsymbol{\eta}}}^*_c \tag{32}$$

follows a chi-squared distribution, $\chi^2_{W_c}$, with W_c degrees of freedom. If $\omega_c > \chi^2(\alpha, W_c)$, H^c_0 will be rejected under asymptotic α. Here, $\chi^2(\alpha, W_c)$ denotes the upper $100\alpha\%$ point of $\chi^2_{W_c}$. When H^c_0 is not rejected, it indicates that there is no significant evidence to reject the null hypothesis that the restricted loading elements are simultaneously equal to zeros, i.e., it cannot reject the null hypothesis that the rotated factor loading vectors match the SPVs specified by $\mathbf{T}_c$. Thus, the variation sources combination c will be identified as the actual variation sources.

In a summary, the variation sources identification is based on the EDFA and the statistical test of the restricted loading vectors. The general procedure is illustrated in Fig. 3, and it includes four major steps as follows:

- **S1**: The principal component decomposition will be performed based on the KPC measurement data and sample variance–covariance matrix, $\mathbf{S}_\mathbf{y}$. The number of significant variation sources, s, will be determined according to AIC. Initial loading vectors in $\hat{\mathbf{L}}$ will be calculated from eigenvalues and eigenvectors of $\mathbf{S}_\mathbf{y}$.
- **S2**: Initial loading vectors will be rotated with IVGFR and the given $\mathbf{T}_c$. The rotated loading matrix, $\hat{\mathbf{L}}^*_c$, rotation matrix, $\mathbf{R}_c$, and the optimization index, Q_c, will be used to evaluate the sampling variability of $\hat{\mathbf{L}}^*_c$ in **S3**.
- **S3**: Asymptotic variance–covariance matrix of $\hat{\mathbf{L}}^*_c$ will be calculated according to Eq. (11). The partial derivatives of the rotation function h_c are derived by the general implicit differentiation method and the specific constraint function for IVGFR, as defined in Eqs. (22)–(26).
- **S4**: The asymptotic variance–covariance matrix of the rotated factor loading elements will be used to conduct a statistical test to check the match between the restricted loading vectors, as defined in Eq. (29), and the predefined IVs. When the null hypothesis in Eq. (31) is not rejected, the variation sources of combination c are identified as the actual variation sources. Otherwise, the procedure will continue to explore other IV combinations.

3 Case Study

A case study on the process shown in Fig. 1 is conducted to demonstrate the capability of the proposed approach. Table 1

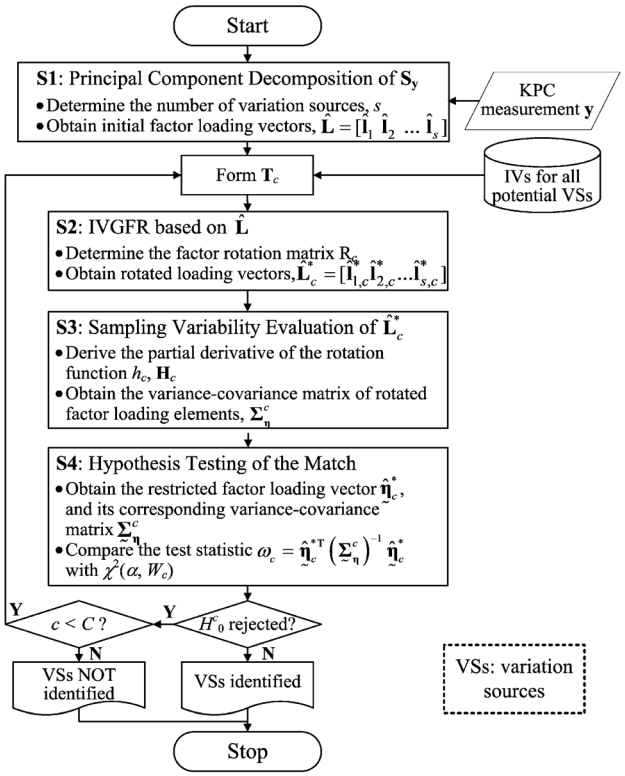

Fig. 3 The procedure of EDFA based variation source identification

summarizes the process by listing the assembly operations and the fixturing schemes. The potential variation sources are the random variations of the four-way pins along X-direction and Z-direction, and that of the two-way pins along Z-direction. For simplicity, only the fixture locator pins used in stages 1 and 2 are considered and thus there are 12 potential variation sources. According to the engineering knowledge of the relationships between variation sources and KPC measurements, 12 IVs are formed. For instance, the IV for the variation source P_1 along Z-direction is $\boldsymbol{\tau}_{P_{1\_z}} = [\mathbf{1}^{\mathrm{T}}_{32}\mathbf{0}^{\mathrm{T}}_6]^{\mathrm{T}}$, while that for the variation sources P_3 along Z-direction is $\boldsymbol{\tau}_{P_{3\_z}} = [\,\mathbf{0}^{\mathrm{T}}_4\ \ \mathbf{1}^{\mathrm{T}}_{28}\ \ \mathbf{0}^{\mathrm{T}}_6\,]^{\mathrm{T}}$.

A Monte Carlo simulation is performed to generate measurement data based on the linear model (1), where the matrix $\boldsymbol{\Gamma}$ is derived with the state space modeling technique introduced in Ref. [9]. Corresponding to the 12 potential variation sources, matrix $\boldsymbol{\Gamma}$ contains 12 SPVs, describing the impacts of the variation sources on the variations of KPC measurements. The input vector $\mathbf{u}$ follows a normal distribution, i.e., $\mathbf{u} \sim N(\mathbf{0}_{12}, \boldsymbol{\Sigma}_{\mathbf{u}})$. It is assumed that no variation source is manifested as a mean-shift, i.e., $\boldsymbol{\mu}_{\mathbf{u}} = \mathbf{0}_{12}$. The diagonal elements of matrix $\boldsymbol{\Sigma}_{\mathbf{u}}$ are the variances of the variation sources, with the value of 0.1 denoting the normal inherent variation level specified by the fixture design tolerance. In this case study, the four-way pin P_1 used in the first stage and the four-way pin P_3 used in the second stage introduce abnormally large variances, both along Z-directions, as shown in Fig. 1. Correspondingly, the second (P_{1_Z}) and the fifth (P_{3_Z}) diagonal elements of $\boldsymbol{\Sigma}_{\mathbf{u}}$ are 0.6 and 0.5, respectively, whereas the other diagonal elements of $\boldsymbol{\Sigma}_{\mathbf{u}}$ are set to be 0.1. The measurement error vector $\mathbf{v}$ follows a normal distribution, i.e., $\mathbf{v} \sim N(\mathbf{0}_{38}, \boldsymbol{\Sigma}_{\mathbf{v}})$, where $\boldsymbol{\Sigma}_{\mathbf{v}}$ is a 38×38 diagonal matrix with all diagonal elements equal to 0.001.

Table 1 Summary of the three-stage assembly process

Stage	Fixture	Operations
1	Fix part A by P_1 and P_2 Fix part B by P_3 and P_4	Assemble parts A and B
2	Fix subassembly A&B by P_5 and P_6 Fix part C by P_7 and P_8	Assemble subassembly A&B and part C
3	Fix side aperture by P_9 and P_{10}	Measure 19 features (F_1–F_{19}) on the side aperture

Table 2 Rotated factor loading vectors and their corresponding IVs

Variation source 1, $\hat{\mathbf{l}}^*_{1,14}$						Variation source 2, $\hat{\mathbf{l}}^*_{2,14}$					
j	$\hat{l}^*_{j1,14}$	$\tau_{P_{1\_z}}$	j	$\hat{l}^*_{j1,14}$	$\tau_{P_{1\_z}}$	j	$\hat{l}^*_{j2,14}$	$\tau_{P_{3\_z}}$	j	$\hat{l}^*_{j2,14}$	$\tau_{P_{3\_z}}$
1	0.0010	1	20	0.3347	1	1	0.0022	0	20	−0.2783	1
2	0.2473	1	21	−0.0135	1	2	−0.0034	0	21	0.1881	1
3	−0.2293	1	22	0.1206	1	3	0.0038	0	22	−0.0886	1
4	0.7097	1	23	−0.0942	1	4	−0.0067	0	23	0.2374	1
5	−0.0139	1	24	0.1627	1	5	0.1771	1	24	−0.1267	1
6	0.7041	1	25	−0.0905	1	6	−0.5946	1	25	0.2662	1
7	0.1326	1	26	0.3406	1	7	0.0107	1	26	−0.2808	1
8	0.7101	1	27	−0.0148	1	8	−0.6009	1	27	0.1888	1
9	0.2080	1	28	0.3658	1	9	−0.0453	1	28	−0.3031	1
10	0.5859	1	29	−0.0926	1	10	−0.4924	1	29	0.2484	1
11	0.2446	1	30	0.4292	1	11	−0.0342	1	30	−0.3617	1
12	0.5046	1	31	−0.0930	1	12	−0.4260	1	31	0.2168	1
13	0.2792	1	32	0.4863	1	13	−0.0643	1	32	−0.4053	1
14	0.4207	1	33	−0.0284	0	14	−0.3499	1	33	−0.0272	0
15	0.2017	1	34	−0.0117	0	15	−0.0487	1	34	−0.0116	0
16	0.3422	1	35	−0.0236	0	16	−0.2865	1	35	−0.0279	0
17	0.2833	1	36	−0.0060	0	17	−0.0864	1	36	−0.0040	0
18	0.2904	1	37	−0.0162	0	18	−0.2364	1	37	−0.0154	0
19	0.1463	1	38	−0.0047	0	19	0.0102	1	38	0.0001	0

In order to demonstrate the effectiveness of the proposed methodology in identifying multiple variation sources, a sample of 150 observations (cars) are simulated with above parameters. The sample covariance is denoted as $\mathbf{S}_{150}$. Following the procedure proposed in Sec. 2.2, the EDFA was conducted to identify the variation sources by estimating the scaled SPVs. The number of significant variation sources that are detected based on AIC criterion is equal to 2 (i.e., $s = 2$). When the combination of the second (P_{1_z}) and the fifth (P_{3_z}) potential variation sources are selected to form a $\mathbf{T}_c$, $c = 14$, the rotated factor loading vectors are obtained and listed in Table 2, together with their corresponding IVs. According to the IVs, $\boldsymbol{\tau}_{P_{1\_z}}$ and $\boldsymbol{\tau}_{P_{3\_z}}$, there are W_{14} ($W_{14} = 16$) restricted elements in $\hat{\mathbf{l}}^*_{1,14}$ and $\hat{\mathbf{l}}^*_{2,14}$, and thus the restricted loading vector, $\hat{\boldsymbol{\eta}}^*_{14}$, is

$$\hat{\boldsymbol{\eta}}^*_{14} = [-0.0284, -0.0117, -0.0236, -0.0060, -0.0162, -0.0047, 0.0022, -0.0034, 0.0038, -0.0067, -0.0272, -0.0116, -0.0279, -0.0040, -0.0154, 0.0001]^{\mathrm{T}}$$

The asymptotic variance–covariance matrix of the restricted loading elements, $\boldsymbol{\Sigma}^{14}_{\eta}$, is given in Appendix A. The calculation of test statistic gives $\omega_{14} = \hat{\boldsymbol{\eta}}^{*\mathrm{T}}_{14} \left(\boldsymbol{\Sigma}^{14}_{\eta}\right)^{-1} \hat{\boldsymbol{\eta}}^*_{14} = 20.9157$, and the critical value at $\alpha = 0.05$ is $\chi^2(\alpha, W_{14}) = \chi^2(0.05, 16) = 26.2962$. Thus, the null hypothesis that H^c_0: $\boldsymbol{\eta}^*_{14} = \mathbf{0}$ cannot be rejected, and P_{1_z} and P_{3_z} are identified as the actual variation sources.

The analytically derived asymptotic variance–covariance matrix of the restricted loading vector is also validated with a simulation of 10,000 replications. The aforementioned sample covariance $\mathbf{S}_{150}$ is used as a population variance–covariance matrix of $\mathbf{y}$ to generate measurements, in which EDFA is performed 10,000 times with given $\boldsymbol{\tau}_{P_{1\_z}}$ and $\boldsymbol{\tau}_{P_{3\_z}}$. The rotated loading vectors are recorded and the sample variance–covariance matrix of

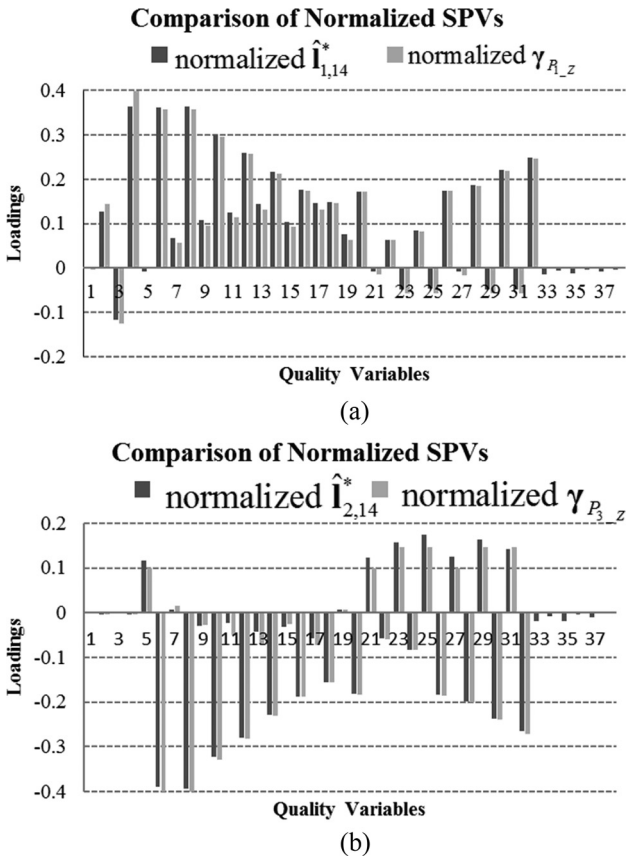

Fig. 4 Comparison of standardized SPVs

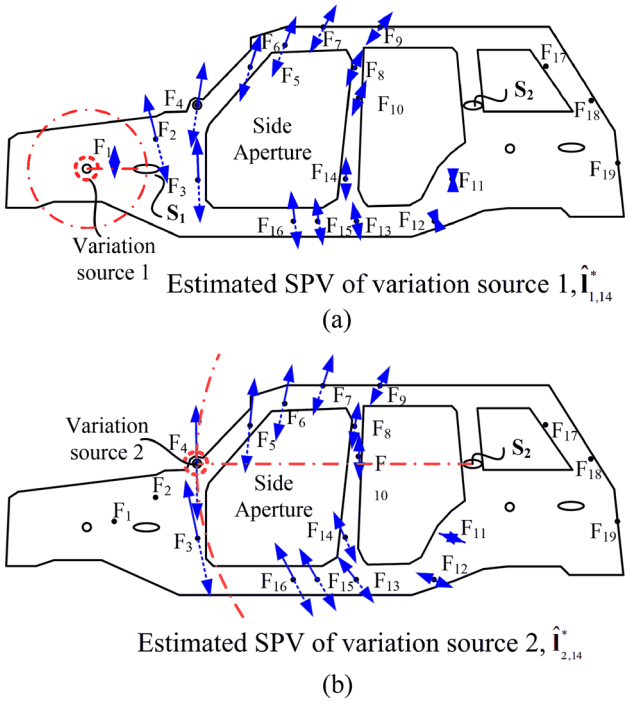

Fig. 5 Visualization of estimated SPVs

the 10,000 restricted loading vectors, $\mathbf{S}^{14}_{\sim\eta}$, are calculated and presented in Appendix B. It can be seen that the true values of $\mathbf{\Sigma}^{14}_{\sim\eta}$ matches $\mathbf{S}^{14}_{\sim\eta}$ with a reasonable accuracy.

As shown in Fig. 4, the standardized rotated factor loading vectors calculated from $\hat{\mathbf{I}}^*_{1,14}$ and $\hat{\mathbf{I}}^*_{2,14}$ are compared with the standardized true SPVs, which are used to simulate the measurement data. This visual comparison shows that the rotated factor loading vectors match the true SPVs very well. The estimated SPVs, $\hat{\mathbf{I}}^*_{1,14}$, and $\hat{\mathbf{I}}^*_{2,14}$, are also visualized in Fig. 5. The scaled estimated SPV of variation source 1, $\hat{\mathbf{I}}^*_{1,14}$, shows that the two features on part A, F_1 and F_2, deviate from their nominal positions along circles centered at the hole S_1, whereas the features on part B, F_3–F_{16}, deviate along circles centered at the hole S_2. This pattern indicates that P_1 used at stage 1 has an abnormally large variation along Z-direction. The scaled estimated SPV of variation source 2, $\hat{\mathbf{I}}^*_{2,14}$, shows that all the features on part B, F_3–F_{16}, deviate from their nominal positions along circles centered at slot S_2, while the features on Part A and Part C are not affected. This pattern indicates that P_3 used in stage 1 has an abnormally large variation along Z direction. In practice, although their true SPVs are unknown, the variation sources identification result can still be justified by visualizing and interpreting the geometric implications of the estimated SPVs. Those estimated SPVs can also be used to update engineering domain knowledge about the complex interrelationships between process variation sources and KPC variances.

The robustness of the proposed method (denoted as method 2) to sample estimation uncertainty was compared with that of the method introduced by Liu et al. [19] (denoted as method 1). Different from method 2, method 1 does not explicitly consider the impact of sampling uncertainty. Identification of variation sources, P_{1_z} and P_{3_z}, were performed for a set of seven different scenarios with different sample size of 50, 100, 150, 250, 500, 1000, and 2000, respectively. In each scenario, 1000 replicates of the variation sources identification were conducted using these two methods. Their performances are compared with respect to the misidentification rate, which is defined as the number of misidentified cases over the total number of replicates. The comparison results are shown in Fig. 6. It can be seen that the proposed statistical-testing-based method, method 2, consistently outperforms method 1, especially under a small sample size. Specifically, when the sample size is large, e.g., $n = 2000$, the methods 1 and 2 have comparable performance. However, when the sample size is small, e.g., $n = 50$, the misidentification rate of method 1 is significantly larger than that of method 2. This is because the variances and/or covariances of the rotated factor loading elements are inversely related to the sample size n. A small sample size leads to a large variance of the loading estimation, which may make the rotated loading vectors significantly deviate from the true SPV. As a result, Q_c, which corresponds to the correct combination of variation sources, will high likely deviate significantly from zero. As a result, method 1 deteriorates to a high misidentification rate over 20%. In contrast, the proposed method 2 can explicitly consider the sampling uncertainty by quantifying its variation with

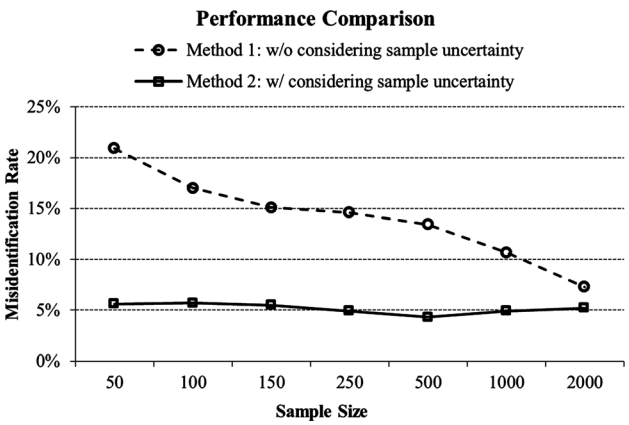

Fig. 6 Performance comparison in terms of robustness to sample uncertainty

the asymptotic variance–covariance coefficients, thus, achieving the robust misidentification rate around 6%.

4 Conclusion

EDFA is an statistical method for identifying the actual variation sources in MMPs by integrating qualitative engineering domain knowledge and multivariate statistical analysis. However, when the sample size of the measurement data is limited by the cost and time constraints, its effectiveness will be impaired due to sample estimation uncertainty. This paper investigates the asymptotic variability of the rotated factor loading elements derived from sample variance–covariance matrix. The asymptotic multivariate distribution and corresponding parameters, i.e., mean vector and variance–covariance matrix of rotated factor loading elements, are analytically derived for the IVGFR method. Based on this derivation, variation sources identification is formulated as an asymptotic statistical test on the hypothesized match between the rotated factor loading elements and the restricted elements predefined in IVs. A procedure based on the EDFA and the statistical testing is proposed for the variation source identification in MMPs. The proposed method will significantly reduce the misidentification rate, especially when the sample size of measurement data is small. The effectiveness and the advantages of the proposed method have been demonstrated by a case study of a three-stage assembly process.

The identifiability or diagnosability of the method may be impaired by the special structure of the IVs. For instance, if the restricted elements in the IV of a potential variation source are a subset of that in the IV of another variation source, or two IVs are different in very few (e.g., only one) elements, both variation sources may be identified as the actual variation sources but the misidentification rate will be increased. Specifically, it is possible to generate two types of errors, i.e., (i) the null hypothesis corresponding to the IV of the actual variation source is rejected, or (ii) the null hypothesis corresponding to the IV of a nonfaulty variation source is not rejected. These two types of errors are equivalent to the type-I error and type-II error, respectively, and thus their probabilities can be evaluated accordingly. One solution of increasing the sensitivity of the test is to adjust the level of the test based on ω_c defined in Eq. (32). Future research is needed to identify the potential combinations of such unidentifiable variation sources subsets and the corresponding IVs.

Acknowledgment

The authors gratefully acknowledge the financial support from the NSF Grants (CMMI-0825438 and CMMI-1100949). The authors also thank the anonymous reviewers for their constructive comments.

Nomenclature

$\mathbf{y}$ = a $p \times 1$ vector containing random deviations of p KPCs
$\mathbf{S}_\mathbf{y}$ = sample covariance matrix of $\mathbf{y}$
$\mathbf{u}_s$ = an $s \times 1$ vector containing random deviations of s process variation sources that actually present in the process
$\mathbf{\Gamma}_s$ = a $p \times s$ matrix with each column a spatial pattern vector of a variation source
p = the number of KPCs
n = the sample size
s = the number of variation sources that actually present in the process
M = the number of potential variation sources
c = the index of a combination of s potential variation sources
C = the total number of combinations when choosing s out of M variation sources
$\mathbf{T}_c$ = a $p \times s$ matrix with the indicator vectors of the variation sources in combination c
$\mathbf{l}_r$ = a $p \times 1$ initial factor loading vector, and $\mathbf{l}_r$ is orthogonal to $\mathbf{l}_t$ for $r \neq t$, $r, t = 1, 2, \ldots, s$
$\mathbf{L}$ = a $p \times s$ initial loading matrix of $\mathbf{l}_r$'s
$\hat{\mathbf{l}}_r$ = a $p \times 1$ initial factor loading vector estimated from $\mathbf{S}_\mathbf{y}$
$\hat{\mathbf{L}}$ = a $p \times s$ initial loading matrix estimated from $\mathbf{S}_\mathbf{y}$
$\mathbf{l}^*_{r,c}$ = a $p \times 1$ rotated factor loading vector, $r = 1, 2, \ldots, s$, given c
$\mathbf{L}^*_c$ = a $p \times s$ rotated loading matrix of $\mathbf{l}^*_{r,c}$'s
$\hat{\mathbf{l}}^*_{r,c}$ = a $p \times 1$ rotated factor loading vector estimated from $\mathbf{S}_\mathbf{y}$, given c
$\hat{\mathbf{L}}^*_c$ = a $p \times s$ rotated loading matrix estimated from $\mathbf{S}_\mathbf{y}$, given c
$\mathbf{R}_c$ = rotation matrix, given c
$\boldsymbol{\tau}_m$ = a $p \times 1$ indicator vector, $m = 1, 2, \ldots, M$
$\hat{\underset{\sim}{\boldsymbol{\eta}}}^*_c$ = restricted loading vector, given c
$\underset{\sim}{\mathbf{\Sigma}}^c_{\boldsymbol{\eta}}$ = the asymptotic variance–covariance matrix of $\hat{\underset{\sim}{\boldsymbol{\eta}}}^*_c$, given c
SPV = spatial pattern vector
EDFA = engineering-driven factor analysis
IV = indicator vector
IVGFR = indicator vector guided factor rotation

Appendix A: The Variance-Covariance Matrix of the Restricted Loading Vector

The variance–covariance matrix analytically derived for the restricted loading vector is

$$\underset{\sim}{\mathbf{\Sigma}}^{14}_{\boldsymbol{\eta}} = 10^{-4} \times \begin{bmatrix}
3.133 & 1.687 & 2.575 & 0.814 & 1.518 & 0.337 & 0.002 & -0.057 & 0.050 & 38; -0.151 & 0.179 & 0.087 & 0.152 & 0.043 & 0.102 & 0.021 \\
1.687 & 2.528 & 0.788 & 1.153 & -0.830 & 0.366 & 0.001 & -0.020 & 0.016 & -0.046 & 0.101 & 0.067 & 0.076 & 0.034 & 0.034 & 0.014 \\
2.575 & 0.788 & 2.405 & 0.397 & 1.913 & 0.209 & 0.002 & -0.038 & 0.033 & -0.100 & 0.140 & 0.058 & 0.119 & 0.030 & 0.088 & 0.015 \\
0.814 & 1.153 & 0.397 & 0.563 & -0.346 & 0.166 & 0.001 & -0.011 & 0.009 & -0.027 & 0.052 & 0.035 & 0.040 & 0.015 & 0.018 & 0.007 \\
1.518 & -0.830 & 1.913 & -0.346 & 2.520 & -0.024 & 0.002 & -0.031 & 0.028 & -0.087 & 0.089 & 0.020 & 0.083 & 0.011 & 0.071 & 0.007 \\
0.337 & 0.366 & 0.209 & 0.166 & -0.024 & 0.087 & 0.000 & -0.011 & 0.010 & -0.030 & 0.025 & 0.014 & 0.020 & 0.007 & 0.011 & 0.001 \\
0.002 & 0.001 & 0.002 & 0.001 & 0.002 & 0.000 & 0.025 & -0.003 & 0.003 & -0.007 & 0.021 & 0.019 & 0.011 & 0.008 & -0.005 & 0.005 \\
-0.057 & -0.020 & -0.038 & -0.011 & -0.031 & -0.011 & -0.003 & 2.522 & -2.197 & 7.008 & -0.509 & -0.095 & -0.461 & -0.040 & -0.365 & -0.065 \\
0.050 & 0.016 & 0.033 & 0.009 & 0.028 & 0.010 & 0.003 & -2.197 & 1.953 & -6.168 & 0.433 & 0.086 & 0.390 & 0.034 & 0.300 & 0.056 \\
-0.151 & -0.046 & -0.100 & -0.027 & -0.087 & -0.030 & -0.007 & 7.008 & -6.168 & 19.733 & -1.328 & -0.253 & -1.194 & -0.107 & -0.919 & -0.181 \\
0.179 & 0.101 & 0.140 & 0.052 & 0.089 & 0.025 & 0.021 & -0.509 & 0.433 & -1.328 & 3.438 & 1.850 & 2.829 & 0.893 & 1.668 & 0.372 \\
0.087 & 0.067 & 0.058 & 0.035 & 0.020 & 0.014 & 0.019 & -0.095 & 0.086 & -0.253 & 1.850 & 2.677 & 0.900 & 1.223 & -0.815 & 0.391 \\
0.152 & 0.076 & 0.119 & 0.040 & 0.083 & 0.020 & 0.011 & -0.461 & 0.390 & -1.194 & 2.829 & 0.900 & 2.623 & 0.452 & 2.061 & 0.236 \\
0.043 & 0.034 & 0.030 & 0.015 & 0.011 & 0.007 & 0.008 & -0.040 & 0.034 & -0.107 & 0.893 & 1.223 & 0.452 & 0.595 & -0.337 & 0.178 \\
0.102 & 0.034 & 0.088 & 0.018 & 0.071 & 0.011 & -0.005 & -0.365 & 0.300 & -0.919 & 1.668 & -0.815 & 2.061 & -0.337 & 2.662 & -0.014 \\
0.021 & 0.014 & 0.015 & 0.007 & 0.007 & 0.001 & 0.005 & -0.065 & 0.056 & -0.181 & 0.372 & 0.391 & 0.236 & 0.178 & -0.014 & 0.091
\end{bmatrix}$$

Appendix B: Validation of the Covariance Estimation

The variance–covariance matrix of the restricted loading vector from simulation of 10,000 replicates is

$$\underset{\sim}{\mathbf{S}}_{\eta}^{14} = 10^{-4} \times \begin{bmatrix}
3.446 & 1.918 & 2.802 & 0.926 & 1.586 & 0.373 & 0.002 & -0.053 & 0.048 & -0.150 & 0.172 & 0.086 & 0.151 & 0.041 & 0.104 & 0.020 \\
1.918 & 2.748 & 0.920 & 1.256 & -0.716 & 0.398 & 0.001 & -0.019 & 0.015 & -0.044 & 0.082 & 0.062 & 0.071 & 0.032 & 0.036 & 0.014 \\
2.802 & 0.920 & 2.578 & 0.462 & 1.970 & 0.233 & 0.002 & -0.038 & 0.030 & -0.099 & 0.139 & 0.053 & 0.098 & 0.029 & 0.077 & 0.014 \\
0.926 & 1.256 & 0.462 & 0.614 & -0.278 & 0.181 & 0.001 & -0.011 & 0.009 & -0.026 & 0.044 & 0.035 & 0.038 & 0.014 & 0.019 & 0.006 \\
1.586 & -0.716 & 1.970 & -0.278 & 2.533 & -0.023 & 0.003 & -0.029 & 0.028 & -0.086 & 0.081 & 0.018 & 0.080 & 0.009 & 0.096 & 0.007 \\
0.373 & 0.398 & 0.233 & 0.181 & -0.023 & 0.094 & 0.000 & -0.011 & 0.010 & -0.030 & 0.021 & 0.013 & 0.017 & 0.007 & 0.012 & 0.001 \\
0.002 & 0.001 & 0.002 & 0.001 & 0.003 & 0.000 & 0.027 & -0.003 & 0.003 & -0.007 & 0.020 & 0.022 & 0.010 & 0.007 & -0.004 & 0.005 \\
-0.053 & -0.019 & -0.038 & -0.011 & -0.029 & -0.011 & -0.003 & 2.343 & -2.248 & 7.183 & -0.570 & -0.092 & -0.436 & -0.037 & -0.330 & -0.060 \\
0.048 & 0.015 & 0.030 & 0.009 & 0.028 & 0.010 & 0.003 & -2.248 & 1.816 & -5.089 & 0.432 & 0.071 & 0.364 & 0.033 & 0.297 & 0.052 \\
-0.150 & -0.044 & -0.099 & -0.026 & -0.086 & -0.030 & -0.007 & 7.183 & -5.089 & 20.457 & -1.157 & -0.222 & -1.073 & -0.100 & -0.888 & -0.190 \\
0.172 & 0.082 & 0.139 & 0.044 & 0.081 & 0.021 & 0.020 & -0.570 & 0.432 & -1.157 & 3.576 & 2.031 & 2.931 & 0.989 & 1.640 & 0.421 \\
0.086 & 0.062 & 0.053 & 0.035 & 0.018 & 0.013 & 0.022 & -0.092 & 0.071 & -0.222 & 2.031 & 3.001 & 0.992 & 1.384 & -0.969 & 0.454 \\
0.151 & 0.071 & 0.098 & 0.038 & 0.080 & 0.017 & 0.010 & -0.436 & 0.364 & -1.073 & 2.931 & 0.992 & 2.715 & 0.502 & 2.073 & 0.268 \\
0.041 & 0.032 & 0.029 & 0.014 & 0.009 & 0.007 & 0.007 & -0.037 & 0.033 & -0.100 & 0.989 & 1.384 & 0.502 & 0.680 & -0.414 & 0.209 \\
0.104 & 0.036 & 0.077 & 0.019 & 0.096 & 0.012 & -0.004 & -0.330 & 0.297 & -0.888 & 1.640 & -0.969 & 2.073 & -0.414 & 2.753 & -0.015 \\
0.020 & 0.014 & 0.014 & 0.006 & 0.007 & 0.001 & 0.005 & -0.060 & 0.052 & -0.190 & 0.421 & 0.454 & 0.268 & 0.209 & -0.015 & 0.108
\end{bmatrix}$$

References

[1] Shi, J., 2006, *Stream of Variation Modeling and Analysis for Multistage Manufacturing Processes*, CRC Press, Taylor & Francis Group, Boca Raton, FL, p. 469.

[2] Wolbrecht, E., D'Ambrosio, B., Paasch, R., and Kirby, D., 2000, "Monitoring and Diagnosis of a Multistage Manufacturing Process Using Bayesian Networks," Artif. Intell. Eng. Des. Anal. Manuf., **14**(1), pp. 53–67. Available at http://journals.cambridge.org/action/displayAbstract?fromPage=online&aid=38559

[3] Ceglarek, D., and Shi, J., 1996, "Fixture Failure Diagnosis for Auto Body Assembly Using Pattern Recognition," ASME J. Eng. Ind., **118**, pp. 55–65.

[4] Li, Z., and Zhou, S., 2006, "Robust Method of Multiple Variation Sources Identification in Manufacturing Processes For Quality Improvement," ASME J. Manuf. Sci. Eng., **128**, pp. 326–336.

[5] Apley, D. W., and Shi, J., 2001, "A Factor-Analysis Method for Diagnosing Variability in Multivariate Manufacturing Processes," Technometrics, **43**(1), pp. 84–95.

[6] Liu, J., Li, J., and Shi, J., 2005, "Engineering Driven Cause-Effect Modeling and Statistical Analysis for Multi-Operational Machining Process Diagnosis," Trans. NAMRI/SME, **33**, pp. 65–72.

[7] Apley, D. W., and Lee, H. Y., 2003, "Identifying Spatial Variation Patterns in Multivariate Manufacturing Processes: A Blind Separation Approach," Technometrics, **45**(3), pp. 187–198.

[8] Jin, J., and Shi, J., 1999, "State Space Modeling of Sheet Metal Assembly for Dimensional Control," ASME J. Manuf. Sci. Eng., **121**, pp. 756–762.

[9] Liu, J., Jin, J., and Shi, J., 2010, "State Space Modeling for 3-D Variation Propagation in Rigid-Body Multistage Assembly Processes," IEEE Trans. Autom. Sci. Eng., **7**(4), pp. 724–735.

[10] Mantripragada, R., and Whitney, D. E., 1999, "Modeling and Controlling Variation Propagation in Mechanical Assemblies Using State Transition Models," IEEE Trans. Rob. Autom., **15**(1), pp. 124–140.

[11] Zhou, S., Huang, Q., and Shi, J., 2003, "State Space Modeling of Dimensional Variation Propagation in Multistage Machining Process Using Differential Motion Vector," IEEE Trans. Rob. Autom., **19**(2), pp. 296–309.

[12] Li, B., Yu, H., Yang, X., and Hu, Y., 2010, "Variation Analysis and Robust Fixture Design of a Flexible Fixturing System for Sheet Metal Assembly," ASME J. Manuf. Sci. Eng., **132**(4), p. 041014.

[13] Ding, Y., Ceglarek, D., and Shi, J., 2002, "Fault Diagnosis of Multistage Manufacturing Processes by Using State Space Approach," ASME J. Manuf. Sci. Eng., **124**(2), pp. 313–322.

[14] Zhou, S., Chen, Y., and Shi, J., 2004, "Statistical Estimation and Testing for Variation Root-Cause Identification of Multistage Manufacturing Processes," IEEE Trans. Autom. Sci. Eng., **1**(1), pp. 73–83.

[15] Kong, Z., Huang, W., and Oztekin, A., 2009, "Variation Propagation Analysis for Multi-Station Assembly Process With Consideration of GD&T Factors," ASME J. Manuf. Sci. Eng., **131**(5), p. 051010.

[16] Huang, W., Lin, J., Bezdecny, M., Kong, Z., and Ceglarek, D., 2007, "Stream-of-Variation Modeling I: A Generic 3D Variation Model for Rigid Body Assembly in Single Station Assembly Processes," ASME J. Manuf. Sci. Eng., **129**(4), pp. 821–831.

[17] Huang, W., Lin, J., Kong, Z., and Ceglarek, D., 2007, "Stream-of-Variation Modeling II: A Generic 3D Variation Model for Rigid Body Assembly in Multi Station Assembly Processes," ASME J. Manuf. Sci. Eng., **131**(5), **129**(4), pp. 832–842.

[18] Abellan-Nebot, J. V., Liu, J., Subiron, F. R., and Shi, J., 2012, "State Space Modeling of Variation Propagation in Multistation Machining Processes Considering Machining-Induced Variations," ASME J. Manuf. Sci. Eng., **134**, p. 021002.

[19] Liu, J., Shi, J., and Hu, S. J., 2008, "Engineering-Driven Factor Analysis for Variation Source Identification in Multistage Manufacturing Processes," ASME J. Manuf. Sci. Eng., **130**(4), p. 041009.

[20] Kollo, T., and Neudecker, H., 1997, "Asymptotics of Pearson-Hotelling Principal-Component Vectors of Sample Variance and Correlation Matrices," Behaviormetrika, **24**(1), pp. 51–69.

[21] Jin, N., and Zhou, S., 2006, "Signature Construction and Matching for Fault Diagnosis in Manufacturing Processes Through Fault Space Analysis," IIE Trans. Qual. Reliab. Eng., **38**, pp. 341–354.

[22] Lawley, D. N., and Maxwell, A. E., 1971, *Factor Analysis as a Statistical Method*, Butterworths, London, p. 153.

[23] Archer, C. O., and Jennrich, R. I., 1973, "Standard Errors for Rotated Factor Loadings," Psychometrika, **38**(4), pp. 581–592.

[24] Jennrich, R., 1973, "Standard Errors for Obliquely Rotated Factor Loadings," Psychometrika, **38**(4), pp. 593–604.

[25] Ogasawara, H., 2002, "Concise Formulas for the Standard Errors of Component Loading Estimates," Psychometrika, **67**(2), pp. 289–297.

[26] Girshick, M. A., 1939, "On the Sampling Theory of Roots of Determinantal Equations," Ann. Math. Stat., **10**, pp. 203–224.